

# A Model for Metal Adsorption on Montmorillonite

Anne M. L. Kraepiel,<sup>\*1</sup> Klaus Keller,<sup>†</sup> and François M. M. Morel<sup>‡</sup>

<sup>\*</sup>Department of Chemistry, Frick Chemical Laboratory, Princeton University, Princeton, New Jersey 08544; <sup>†</sup>Department of Civil Engineering and Operations Research, Princeton University, Princeton, New Jersey 08544; and <sup>‡</sup>Department of Geosciences, Guyot Hall, Princeton University, New Jersey 08544

Received December 15, 1997; accepted October 24, 1998

**A consistent thermodynamic model is developed for metal sorption on expanding 2:1 layer clays such as montmorillonite. The particle of clay, including lamellae and interlayers, is represented as a porous solid bearing a permanent negative charge (resulting from isomorphous substitution) with an infinite plane interface (i.e., edges) with the solution. Cation exchange occurs inside the clay particle as the result of the negative potential of the clay. Surface complexation reactions take place at the interface whose surface charge and potential are pH dependent. The potential in the bulk of the clay and near the interface, as well as the surface potential–surface charge density relation, are calculated taking into account the effect of the permanent negative charge. The results are discussed and compared with the classic Gouy–Chapman theory. A subroutine (Clayeq) with the new potential–charge relationships is implemented in the thermodynamic equilibrium program Mineql + 3.0 and is used to fit an extensive published experimental data set on adsorption of transition metals on montmorillonite. The model is shown not only to fit satisfactorily all the data, but also to explain specific features of adsorption on clays compared to oxides. In particular, the increase in the surface concentration of protons with decreasing ionic strength is successfully reproduced and the weaker dependence of metal sorption on pH compared to oxides is correctly fitted.** © 1999 Academic Press

**Key Words:** smectites; double-layer; proton adsorption; ion exchange; surface complexation; Donnan equilibrium.

## BACKGROUND

Ion sorption on smectites (expanding 2:1 layer clays with a permanent charge arising from isomorphous substitution) is controlled by two different mechanisms: (i) a pH-independent adsorption, usually attributed to cation exchange in the interlayers and resulting from electrostatic interaction between the ions and the permanent charge, and (ii) a pH-dependent adsorption, thought to result from surface complexation reactions similar to those on oxides (1). On smectites, which have siloxane layers but no gibbsite layers exposed, surface complexation groups are usually assumed to be confined to the edges (2, 3), in accord with spectroscopic evidence (4).

<sup>1</sup> To whom correspondence should be addressed.

Adsorption by cation exchange dominates at low ionic strength or low pH. It can be successfully described by either a Donnan equilibrium model or accumulation of ions in the double layers that develop at the basal planes of the clay lamellae (1, 5). In one case—Donnan equilibrium—the clay particle is conceptualized as a separate homogeneous phase bearing a negative charge (arising from isomorphous substitution). In the other case—accumulation in the double layer—each individual lamella in the clay particle and the double layers that develop in the interlayers are considered. (N.B., a lamella is defined here as an individual layer, i.e., one gibbsite sheet sandwiched between two siloxane sheets; a clay particle is made of a certain number of lamellae and the interlayers between them.)

Independent from the description of cation exchange as resulting from coulombic interactions and quantified by the Donnan or diffuse-layer models, the ion exchange reaction (for example between  $\text{Na}^+$  and  $\text{H}^+$ ) can always be written as



where X is the solid exchanger,  $\text{H}^+$  and  $\text{Na}^+$  represent the ions in solution and  $K_e$  is the mass action law coefficient for the reaction.

Following Fletcher and Sposito (6), it is possible to define  $\text{X}^-$  as a fictitious surface species and write hypothetical complexation reactions:



Such reactions are very similar to surface reactions written in “surface complexation models” (see below) and cation exchange reactions can thus be easily incorporated into such models. As discussed by Dzombak and Hudson (1), the physical interpretation of the activity of  $\text{X}^-$  is model dependent and may, for example, be obtained from the Donnan potential of the clay particle.

The pH-dependent adsorption of metals on clays cannot be accounted for by a purely electrostatic model, but can easily be understood by analogy with the sorption properties of oxides. Because the edges of clays are effectively the surfaces of a mixture of oxides—gibbsite and silica—they should adsorb metals as pure oxide phases do. It is generally assumed that oxygen surface groups have the potential to react with ions in solution to yield surface complexes. These surface reactions may be described with a “surface complexation model” that takes into account both the “intrinsic” affinity of surface sites for solutes and the coulombic interaction between the surface charge and the dissolved ions (7–9).

Adsorption models for clays based on surface complexation models usually involve two distinct types of surface sites at the interface between the solid and the solution: (i)  $\equiv\text{X}^-$  groups bearing a permanent (i.e., pH-independent) charge which account for the cation exchange part of adsorption; (ii) amphoteric  $\equiv\text{SOH}$  groups. The  $\equiv\text{X}^-$  groups are assumed to form very strong surface complexes with the electrolyte cation (e.g.,  $\text{Na}^+$ ) such that free  $\text{X}^-$  never exists and the surface charge is controlled by the protonation/deprotonation of the  $\equiv\text{SOH}$  groups (10–13).

There is one major disadvantage in describing ion exchange reactions, which are known to be chiefly electrostatic in nature, by the way of specific chemical reactions. Namely, the permanent negative charge of the clay is completely neutralized through the formation of a fictitious surface complex with  $\text{Na}^+$  of very high stability. Such models thus cannot account for the influence of the permanent charge on the sorption properties of clays aside from the ion exchange itself. Yet, detailed studies of the electrical double layer on montmorillonite lamellae (14–16) have shown that the negative electrostatic field emanating from the particle faces strongly influences the edge potential. The permanent charge of the clay may thus affect significantly surface complexation of ions on the edges. Unfortunately, the numerical results derived from these studies are too complex to be easily incorporated in a thermodynamic model of adsorption.

Here, we present a general and self-consistent thermodynamic model of cation sorption on montmorillonite where the effect of a permanent negative charge inside the clay particle (due to isomorphous substitution) and the pH-dependent charge on the edges (due to acid-base reactions of surface groups) are both taken into account. After describing the conceptual model, we derive the fundamental equations that relate the electrical potentials in the bulk of the clay particle and on its surface to the permanent internal charge and the variable surface charge. The new model is then used to fit the extensive data set on metal sorption on Na-montmorillonite recently published by Bayens and Bradbury (17) and discussed.

## THEORY

### Conceptual Model

The clay particle is represented as a semi-infinite homogeneous porous solid immersed in an aqueous solution of known ionic strength  $I$  (see Fig. 1). The solid represents both the crystalline layers of the clay (i.e., the lamellae) and the aqueous interlayers; it bears a permanent negative charge  $\rho_{\text{clay}}$ , uniformly distributed, resulting from isomorphous substitution in the structure; the negative potential inside the clay ( $\psi_{\text{clay}}$ ) attracts cations and is responsible for adsorption by cation exchange. This representation of the clay particle is very similar to the “micro-Donnan” system containing a large number of permanent charges homogeneously distributed described by Bolt (5, p. 48); it is also clearly an approximation as the distribution of permanent charges is “smeared” over the lamellae and interlayers instead of being localized on the lamellae as it is in reality. The interface between solid and solution (i.e., only the edges, for in this model, the faces and the interlayers effectively disappear) is taken to be an infinite plane of charge density  $\sigma_o$  and potential  $\psi_o$ , which depends on both  $\rho_{\text{clay}}$  and  $\sigma_o$ . This interface contains reactive surface sites which undergo acid-base and surface complexation reactions. The approximation of the clay particle as an infinite solid, both along the faces and the edges is reasonable since: (i) the edge length is larger than the double-layer thickness ( $\approx 3$  nm at  $I = 0.01$  M) in any particle with more than one lamella; (ii) the finite length of the faces need not be taken into account if, as is the case here, the aspect ratio is high (i.e., face/edge  $> 10$  in one lamella) and the ionic strength is greater than 0.01 M (14, 16).

### Potentials in the Clay, on the Surface and near the Interface

The potential in the bulk of the solid and near the solid–solution interface may be calculated using the Poisson–Boltzmann equation which relates the variations with distance of the electrical potential  $\psi(x)$  to the distribution of charged species. For simplicity, we assume a 1:1 electrolyte ( $[\text{Na}^+] = [\text{ClO}_4^-] = I$ ). The theory of the double double layer has been solved in a number of different systems (18–24), but, to our knowledge, not in the case of a porous solid with both a uniform bulk charge density,  $\rho_p$ , and a surface charge density,  $\sigma_o$ .

On the solution side, the electrical potential and ion concentration vary accordingly to the Gouy–Chapman theory.

From  $x = 0^+ \rightarrow +\infty$ ,

$$\frac{d^2\psi}{dx^2} = - \frac{1000FI(e^{-F\psi/RT} - e^{F\psi/RT})}{\epsilon_w\epsilon_o}, \quad [1]$$

where  $\psi$  is the potential in V,  $I$  is the electrolyte concentration in mol/L (the factor 1000 is included to reconcile the units in meters<sup>3</sup> and liters).  $R$  is the gas constant (8.314 J.mol<sup>-1</sup>.K<sup>-1</sup>),

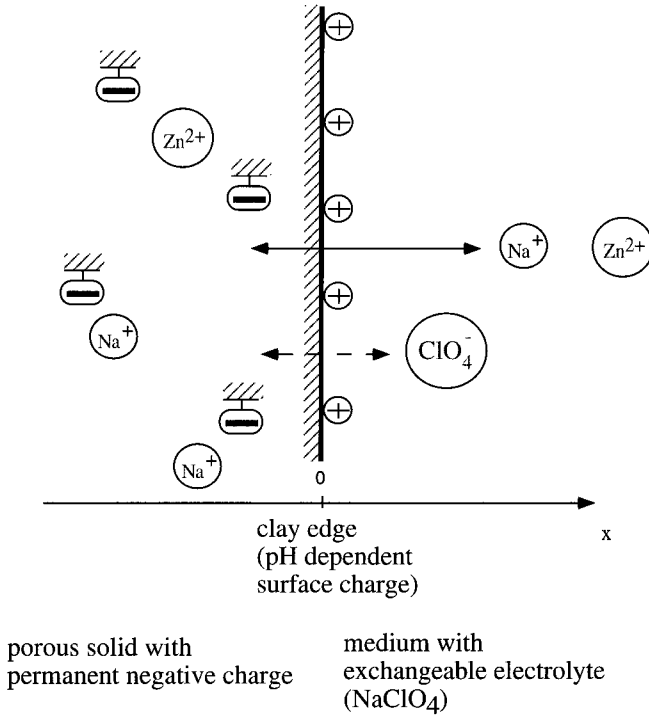


**FIG. 1.** Schematic representation of the conceptual model for montmorillonite. The clay particle (including lamellae and interlayers) is represented as a porous solid bearing a permanent negative charge. This negative charge is exactly balanced by the presence of electrolyte counterions (in this case,  $\text{Na}^+$ ), such that the total net charge of the solid is equal to zero. The negative potential of the clay particle attracts trace metal cations such as  $\text{Zn}^{2+}$  and is responsible for the cation exchange component of adsorption. The clay edges are represented as an infinite surface with sites for surface complexation. The negative potential of the clay influences the surface potential and therefore the surface complexation reactions at the edges.

$T$  is the absolute temperature in K, and  $F$  is the Faraday constant in C.  $\epsilon_0$  is the vacuum permittivity ( $8.854 \cdot 10^{-12} \text{ J}^{-1} \cdot \text{C}^2 \cdot \text{m}^{-1}$ ) and  $\epsilon_w$  (78.5) is the relative permittivity of water.

In the clay, the charge density is the result of both the permanent negative charge and the excess of  $\text{Na}^+$  over  $\text{ClO}_4^-$  ions.

From  $x = -\infty \rightarrow 0^-$ ,

$$\frac{d^2\psi}{dx^2} = -1000 \frac{F\rho_{\text{clay}} + FI(e^{-F\psi/RT} - e^{F\psi/RT})}{\epsilon_c \epsilon_0 (V_p/V_L)}, \quad [2]$$

where  $\rho_{\text{clay}}$  is the permanent charge per solution volume inside the clay particle in  $\text{mol/l}^2$  ( $\rho_{\text{clay}} < 0$ ),  $V_p/V_L$  is the ratio of the

<sup>2</sup> The concentrations in moles per solution volume inside the clay particle are denoted  $\text{mol/l}$ ; the concentrations in moles per total solution volume are indicated as  $\text{mol/L}$ .

total volume of the clay particle to the solution volume inside the clay and normalizes the charge concentration to the solid volume;  $\epsilon_c$  is the relative permittivity of the clay. Equation [2] does not include the negligible effect on the Boltzmann distribution of ions of a possible high internal pressure in the clay particle.

The three boundary conditions are obtained as follows:

(i) in the solution, at infinite distance from the surface, the potential is taken to be zero (as implied in Eq. [1]):

$$\psi = 0 \Big|_{x=+\infty} \quad [3]$$

(ii) the potential is continuous at the interface:

$$\psi(0^-) = \psi(0^+) = \psi_0 \quad [4]$$

(iii) in the clay, at infinite distance from the surface, the system is electrically neutral, which implies (see Eq. [2]):

$$\frac{d^2\psi}{dx^2} \Big|_{x=-\infty} = \frac{d\psi}{dx} \Big|_{x=-\infty} = 0. \quad [5]$$

Equations [1] and [2] are solved to obtain the potential as a function of the distance  $x$  from the surface for any given surface potential  $\psi_0$  (see Fig. 2a). In solution, the potential is the same as in the Gouy–Chapman theory. In the bulk of the clay,  $\psi_{\text{clay}} = \psi(-\infty)$  is obtained as a function of  $\rho_{\text{clay}}$  from Eqs. [2] and [5]:

$$\psi_{\text{clay}} = \frac{RT}{F} \text{arc sinh} \left( \frac{\rho_{\text{clay}}}{2I} \right). \quad [6]$$

At high absolute value of the potential, the concentration of co-ions ( $\text{ClO}_4^-$ ) can be neglected in the bulk of the solid away from the surface. Equation [6] then reduces to

$$e^{-F\psi_{\text{clay}}/RT} = \frac{-\rho_{\text{clay}}}{I}, \quad [7]$$

which is the Donnan expression for the clay potential

$$\psi_{\text{clay}} = \psi_{-\infty} = -2.3 \frac{RT}{F} \log \left( \frac{-\rho_{\text{clay}}}{I} \right). \quad [8]$$

As expected, the potential inside the clay ( $\psi_{\text{clay}}$ ) is negative, like the permanent charge causing it, and depends directly on the ionic strength of the solution (see Fig. 2b). This potential is

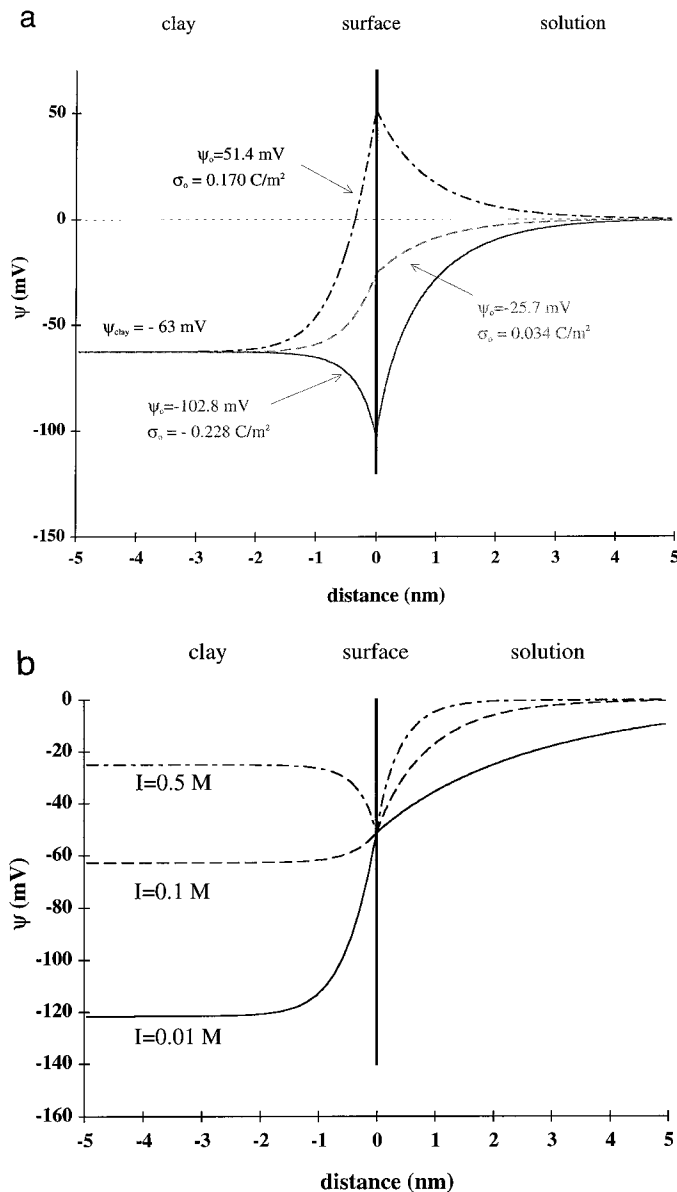


**FIG. 2.**  $\rho_{\text{clay}} = -1.15$  mol/l,  $\epsilon_c/\epsilon_w V_L/V_P = 1$ . (a) Potential as a function of distance in the clay for different surface potentials  $\psi_0$  ( $I = 0.1$  M); (b) Potential as a function of distance for different ionic strengths, the surface potential is fixed at  $\psi_0 = -51$  mV.

of course unaffected by the surface potential or charge whose influence is limited to the near vicinity of the interface.

### Surface Charge and Surface Potential

In the case of the Gouy–Chapman theory (and of the surface complexation models that are directly or indirectly based on it), the surface potential vs surface charge density relation provides a measure of the coulombic interactions between the surface and ionic solutes. In the clay model, the surface potential ( $\psi_0$ )

is a function of the charge density on the edges ( $\sigma_o$ ) and of the permanent charge density in the clay ( $\rho_{\text{clay}}$ ). The expression of electroneutrality, obtained by integrating Eqs. [1] and [2] from  $-\infty$  to  $+\infty$  yields

$$\sigma_o = \epsilon_o \epsilon_c \left. \frac{d\psi}{dx} \right|_{x=0^-} - \epsilon_o \epsilon_w \left. \frac{d\psi}{dx} \right|_{x=0^+} = \sigma_{\text{o clay}} + \sigma_{\text{o G-C}}, \quad [9]$$

where  $\sigma_o$  (C/m<sup>2</sup>) is the surface charge density.

The second term in Eq. [9],  $\sigma_{\text{o G-C}}$ , is that obtained in the Gouy–Chapman theory (to which the clay model simplifies if  $d\psi/dx|_{x=0^-} = 0$ —not if  $\psi_{\text{clay}} = 0$ ) and is calculated by multiplying both sides of Eq. [1] by  $d\psi/dx$  and integrating from 0 to  $+\infty$ :

$$\sigma_{\text{o G-C}} = (8RT\epsilon_w\epsilon_o^*1000)^{1/2} * I^{1/2} * \sinh(F\psi_0/2RT). \quad [10]$$

$\sigma_{\text{o clay}}$  is obtained in a similar way from Eq. [2] by integrating from  $-\infty$  to 0 and by imposing  $\psi(-\infty) = \psi_{\text{clay}}$  as a boundary condition,

$$\begin{aligned} \sigma_{\text{o clay}} = \text{sign} * \left( \frac{8RT\epsilon_o\epsilon_c}{2} \right)^{0.5} \left( \frac{V_L}{V_P} \right)^{0.5} * \left[ 1000I * \left( \cosh\left( \frac{F\psi_0}{RT} \right) \right. \right. \\ \left. \left. - \cosh\left( \frac{F\psi_{\text{clay}}}{RT} \right) \right) + \frac{-1000\rho_{\text{clay}}}{2} * \frac{F}{RT} * (\psi_0 - \psi_{\text{clay}}) \right]^{0.5}, \end{aligned} \quad [11]$$

where  $\text{sign} = +1$  if  $\psi_0 > \psi_{\text{clay}}$ , and  $\text{sign} = -1$  otherwise.

### Sorption of Trace Cations

A simple calculation shows that the variations in potential near the interface, both in solution and in the clay, can usually be neglected for the sorption of a divalent cation. A consistent model thus needs only consider the potential in the bulk of the clay ( $\psi_{\text{clay}}$ ) and at the surface ( $\psi_0$ ) and may ignore the variations in potential near the surface. The sorption of a trace cation  $M^{n+}$  can then be described by superposing reactions inside the solid (cation exchange) and on the surface (surface complexation). Here, we shall consider that the interlayers have no chemical affinity for the cations—including  $H^+$ . As implied by Eqs. [1] and [2],  $Na^+$  and  $ClO_4^-$  (i.e., the electrolyte ions) are considered to be the dominant ions in the system. Clearly, this assumption is verified over most of the pH and ionic strength ranges considered in this study, but breaks down at very low pHs when the proton concentration in solution is higher than the sodium concentration.

**Cation exchange.** Cation exchange results solely from the attraction of cations by the negative potential created inside the clay particle by the permanent negative charge. The extent of

adsorption by cation exchange for a particular cation  $M^{n+}$  can thus be calculated from the potential inside the solid and the concentration of  $M^{n+}$  in solution,

$$\frac{[M^{n+}]_c}{\{M^{n+}\}} = e^{-nF\psi_{\text{clay}}/RT}, \quad [12]$$

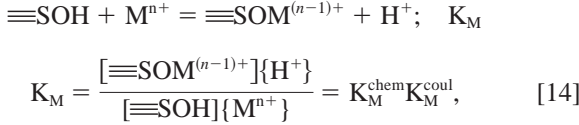
in which  $[M^{n+}]_c$  is the number of moles of  $M^{n+}$  adsorbed by cation exchange per volume solution inside the clay in mol/L (neglecting the activity coefficient, see (5)) and  $\{M^{n+}\}$  is the activity of  $M^{n+}$  in solution in mol/L.

For convenience, the mass law [12] is written using concentration per liter of total solution,

$$\frac{[M^{n+}]_s}{\{M^{n+}\}} = e^{-nF\psi_{\text{clay}}/RT} \frac{m}{V} \frac{1}{d} = {}^{ce}K \quad [13]$$

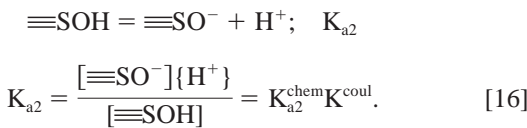
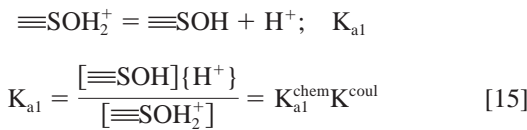
where  $[M^{n+}]_s$  is the number of moles of  $M^{n+}$  adsorbed by cation exchange per total solution volume in mol/L,  $m/V$  is the mass of dry clay per total solution volume in Kg/L and  $d = m/V_L$  is the mass of dry clay per solution volume inside the clay in Kg/l.

*Surface complexation.* The reaction at the interface (surface complexation) of the cation  $M^{n+}$  with a surface site  $\equiv\text{SOH}$  is described as



in which  $[\equiv\text{SOM}^{(n-1)+}]$  and  $[\equiv\text{SOH}]$  are the concentrations of surface sites in mol/L (neglecting again activity coefficients besides the explicit coulombic term; see 25); and  $\{H^+\}$  and  $\{M^{n+}\}$  are the activity of  $H^+$  and  $M^{n+}$  in solution, respectively.

The acid-base reactions at the surface are written as



In this case, the coulombic term ( $K_M^{\text{coul}} = e^{-(n-1)F\psi_o/RT}$  or  $K_{a1}^{\text{coul}} = e^{F\psi_o/RT}$ ) is pH dependent and must be calculated explicitly in each equilibrium calculation.

The surface charge density is calculated from

$$\sigma_o = \frac{F([\equiv\text{SOH}_2^+] - [\equiv\text{SO}^-] + \sum_M (n-1)[\equiv\text{SOM}^{(n-1)+}])}{\frac{m}{V} S}, \quad [17]$$

in which  $S$  is the specific surface area of the clay ( $\text{m}^2/\text{Kg}$ ).

The complete mathematical model for metal adsorption on montmorillonite thus includes for each sorbate a mass law equation for the reaction in the clay particle corresponding to ion exchange and a mass law equation for each surface species considered. In addition, mole balance equations must be obeyed for each component.  $\psi_{\text{clay}}$  is calculated from Eq. [6]. The surface charge density is obtained from Eq. [17] and the surface potential is calculated according to Eqs. [9]–[11].

### APPLICATION TO EXPERIMENTAL DATA

A subroutine, Clayeq1, with the charge–potential relations described previously ( $\psi_{\text{clay}}(\rho_{\text{clay}})$  and  $\sigma_o(\psi_o, \psi_{\text{clay}})$ , see Eqs. [6], [9]–[11]) is implemented in the thermodynamic equilibrium program Mineql + 3.0 and used to fit the set of adsorption data published by Baeyens and Bradbury (17). The sorption edges and isotherms of trace metals (mostly Zn and Ni) were measured on the  $<0.5 \mu\text{m}$  fraction of a conditioned SWy-1 Na-montmorillonite (Crook County, Wyoming). All experiments were conducted in  $\text{NaClO}_4$  electrolyte.

The chemical reactions considered, and their constants, are described in Table 1, while the model parameters are described in Table 2. There are some uncertainties on the value of the ratio  $V_L/V_P$  and the relative permittivity of the clay  $\epsilon_c$ .  $V_L/V_P$  is likely to vary from 0.5 at high ionic strength to almost 1 at low  $I$  (26). The permittivity of the interlayer water may be smaller than the permittivity of bulk water (27) by a factor of two to four, but most solids have a higher permittivity than water. It appears, however, that the model calculations are relatively insensitive to the exact value of the parameters  $V_L/V_P$  and  $\epsilon_c$ ; in the absence of more precise information, we have thus imposed  $\epsilon_c V_L/V_P = \epsilon_w$ . The value of  $d = m/V_L$  is estimated from the Zn sorption edge by assuming that all the Zn adsorption at low pH is due to cation exchange (see Table 2). The specific surface area  $S$  of the interface (i.e., the edges) is taken to be equal to the surface measured by BET by Baeyens and Bradbury (17, 28) and the concentration of permanent charge is fixed equal to the cation exchange capacity (17).

The data were fitted assuming two types of reactive surface sites: the so-called “strong sites,” which have a high affinity for metals, and are responsible for adsorption at low metal concentrations, and the “weak sites,” which play a role only at high pH or high metal concentrations, when the

**TABLE 1**  
**Chemical Reactions at the Solid Surface and in Solution**

	Clay model	Gouy–Chapman model
$\equiv\text{S}^{\text{W}}\text{OH}_2^+ = \equiv\text{S}^{\text{W}}\text{OH} + \text{H}^+$	$\log K_{a1}^{\text{chem}} = -5.6$	$\log K = -6.2$
$\equiv\text{S}^{\text{W}}\text{OH} = \equiv\text{S}^{\text{W}}\text{O}^- + \text{H}^+$	$\log K_{a2}^{\text{chem}} = -8.7$	$\log K = -8.3$
$\equiv\text{S}^{\text{S}}\text{OH}_2^+ = \equiv\text{S}^{\text{S}}\text{OH} + \text{H}^+$	$\log K_{a1}^{\text{chem}} = -4.5$	
$\equiv\text{S}^{\text{S}}\text{OH} = \equiv\text{S}^{\text{S}}\text{O}^- + \text{H}^+$	$\log K_{a2}^{\text{chem}} = -5.5$	
$\equiv\text{S}^{\text{S}}\text{OH} + \text{Ni}^{2+} = \equiv\text{S}^{\text{S}}\text{ONi}^+ + \text{H}^+$	$\log K^{\text{chem}} = 0.40$	
$\equiv\text{S}^{\text{S}}\text{OH} + \text{Zn}^{2+} = \equiv\text{S}^{\text{S}}\text{OZn}^+ + \text{H}^+$	$\log K^{\text{chem}} = 2.30$	
$\equiv\text{S}^{\text{S}}\text{OH} + \text{Mn}^{2+} = \equiv\text{S}^{\text{S}}\text{OMn}^+ + \text{H}^+$	$\log K^{\text{chem}} = 0.60$	
$\equiv\text{S}^{\text{W}}\text{OH} + \text{Ni}^{2+} = \equiv\text{S}^{\text{W}}\text{ONi}^+ + \text{H}^+$	$\log K^{\text{chem}} = -4.5$	
$\equiv\text{S}^{\text{W}}\text{OH} + \text{Zn}^{2+} = \equiv\text{S}^{\text{W}}\text{OZn}^+ + \text{H}^+$	$\log K^{\text{chem}} = -3.2$	

*Note.* The soluble hydrolysis complexes of the metal ions at high pH are included in all the model calculations; the complexes and their constants can be found in Baes and Mesmer (31). The calculated curves shown in the figures are obtained by systematically including the reactions involving Zn and Mn in this table. The reactions with Ni are included only for the Ni sorption edges and the Ni isotherms. In that case, in the absence of more precise information,  $\text{Ni}_{\text{T}} = 3.10^{-7} M$ , which is the upper limit of the Ni added in the experiments (see Baeyens and Bradbury (17)). The presence of Zn and Mn in the system was not taken into account to calculate the Gouy–Chapman curves in Fig. 6. Including them in the calculations would not change the results significantly.

strong sites are saturated. Because the montmorillonite studied has high intrinsic concentrations of Zn ( $10^{-3}$  mol/Kg) and Mn ( $4.10^{-4}$  mol/Kg) compared to the number of strong sites ( $2.10^{-3}$  mol/Kg), Zn and Mn inventories have to be included in all model simulations. Although the constants

**TABLE 2**  
**Model Parameters**

Model parameters	Value	Source
Surface area (edges) ( $\text{m}^2/\text{g}$ )	35	Measured by BET (17)
$\epsilon_c \frac{V_L}{V_p}$	78.5	Fixed equal to $\epsilon_w$
Concentration of weak sites (mol/Kg)	0.08	Potentiometric data
Concentration of strong sites (mol/Kg)	$2.10^{-3}$	Sorption isotherms
Concentration of permanent charge (eq/Kg)	0.87	Fixed equal to CEC (17)
Ratio of dry solid mass to solution volume inside the solid $d = m/V_L$ (Kg/l)	1.32	Zinc sorption edge <sup>a</sup>

<sup>a</sup>  $d$  is calculated according to

$$\frac{[\text{Na}^+]_c}{\{\text{Na}^+\}} = \frac{\rho_{\text{clay}}}{I} = \frac{\text{CEC} * d}{I} \quad [\text{T1}]$$

$$\left(\frac{[\text{Na}^+]_c}{\{\text{Na}^+\}}\right)^2 = \frac{[\text{Zn}^{2+}]_c}{\{\text{Zn}^{2+}\}} = d.R_d^{\text{CE}}. \quad [\text{T2}]$$

$R_d^{\text{CE}} = (\text{moles of Zn adsorbed by cation exchange/mass of dry clay})/(\text{moles of Zn in solution})$ .

$$[\text{T1}] + [\text{T2}] \Rightarrow : d = \frac{R_d^{\text{CE}} * I^2}{\text{CEC}^2}.$$

for the chemical reactions detailed in Table 1 are thus interdependent, a first set of adsorption constants may be obtained as follows: (i) the cation exchange parameters (see footnote of Table 2) are obtained from the Zn sorption edge at low pH; (ii) fitting of the titration data at  $I = 0.5 M$  yields the acid-base constants for the weak sites; (iii) the complexation constants for  $\text{H}^+$ ,  $\text{Zn}^{2+}$ ,  $\text{Mn}^{2+}$ , and  $\text{Ni}^{2+}$  with the strong sites result from fitting the sorption edges of Zn ( $I = 0.1 M$ ), Mn ( $I = 0.5 M$ ) and, Ni ( $I = 0.1 M$ ). The complexation constants for the weak sites with Zn and Ni are obtained by fitting the sorption isotherms of Zn and Ni.

### Cation Exchange

For the same ionic strength ( $I = 0.1 M$ ), Zn and Ni show the same extent of adsorption at low pH, even if their sorption edges are clearly different at higher pH (see Figs. 3 and 4). The pH-independent regions of the Ni and Zn sorption edges at low pH (attributed to cation exchange) are well predicted by the model for both Zn and Ni at all ionic strengths. It should be noted that adsorption of metals by ion exchange is calculated by the model from the ionic strength and the permanent charge density in the clay particle, which is a classic treatment of ion exchange in a Donnan system but is unusual in the context of a surface complexation model. As expected from a simple Donnan equilibrium, the ratio of adsorbed metal to metal in solution is multiplied by 100 when the ionic strength is divided by 10 (see Eqs. [7] and [13]), and the percentage of adsorbed Ni at low pH increases from 10% at  $I = 0.1 M$  to 90% at  $I = 0.01 M$ . The success of the model is an *a posteriori* justification of the treatment of cation exchange as a purely electrostatic process in this system.

### Potentiometric Data

As expected, the proton concentration of the clay edges decreases as pH increases, with a  $\text{pH}_{\text{zsc}}$  (pH of zero surface charge) around 7 (see Fig. 5). In spite of some noise in the data at low and high pH, the surface charge density seems to reach a saturation value that can be used to estimate the total number of surface sites:  $[\equiv\text{S}^{\text{w}}\text{OH}]_T = 0.08 \text{ mol/Kg}$ . The two  $\text{pK}_a$ 's for the surface sites obey the equation

$$\text{pH}_{\text{zsc}} = \frac{1}{2} (\text{pK}_{a1} + \text{pK}_{a2}) - \frac{1}{2.3} \frac{F\psi_{\text{zsc}}}{RT}, \quad [18]$$

where  $\psi_{\text{zsc}}$  is the surface potential such as  $\sigma_o = 0$ . The best fits of the titration data at  $I = 0.5 \text{ M}$  and  $I = 0.1 \text{ M}$  were obtained for  $\log K_{a1} = -5.6$  and  $\log K_{a2} = -8.7$  (see Table 1).

Except at very low pH, the surface charge density is higher at  $I = 0.1 \text{ M}$  than at  $I = 0.5 \text{ M}$  for a given pH. This feature cannot be reproduced by a classic Gouy–Chapman model, but is correctly described by the clay model. This is because, in the clay model, the pH range where  $\psi_o$  increases with  $I$  ( $\text{pH} > \text{pH}^{\text{crit}}$ ) is wider than in the Gouy–Chapman model ( $\text{pH} > \text{pH}_{\text{zsc}}$ ) (see Fig. 6). In the clay model, decreasing  $I$  increases the absolute value of the (negative) internal clay potential as well as decreasing the shielding of the surface charges. The net effect of changing  $I$  on the surface potential (at a given surface charge density) thus depends on the relative sign and magni-

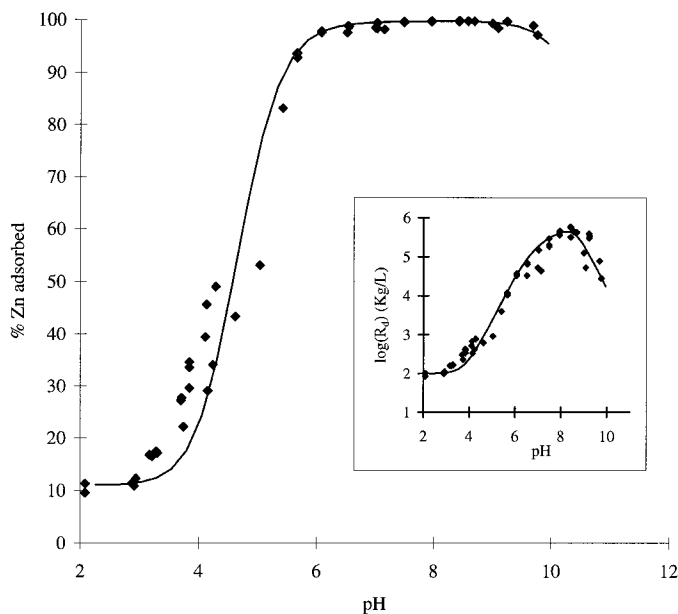


**FIG. 3.** Zn sorption edge at  $I = 0.1 \text{ M}$ . The diamonds are from Baeyens and Bradbury (17). The full line is calculated with Clayeq1 with  $m/V = \text{mass of dry clay/volume solution} = 1.24 \text{ g/L}$ . The fitting parameters are given in Tables 1 and 2. The inset shows the same data on a different scale.  $R_d^{\text{Zn}} = (\text{moles of Zn adsorbed/mass of dry clay})/(\text{moles of Zn in solution})$ .

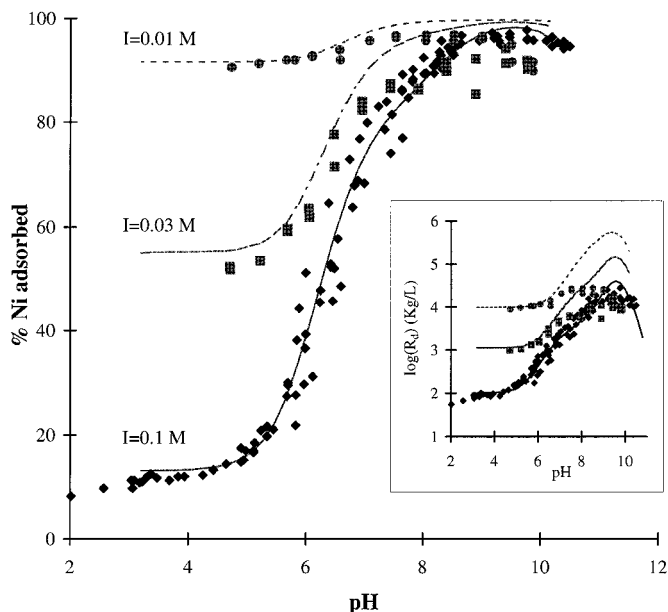


**FIG. 4.** Ni sorption edges at  $I = 0.1 \text{ M}$ ,  $I = 0.03 \text{ M}$  and  $I = 0.01 \text{ M}$ . The diamonds ( $I = 0.1 \text{ M}$ ), the squares ( $I = 0.03 \text{ M}$ ) and the circles ( $I = 0.01 \text{ M}$ ) are from Baeyens and Bradbury (17). The full line (—,  $I = 0.1 \text{ M}$ ,  $m/V = 1.5 \text{ g/L}$ ), the semi-dotted line (- · - · -,  $I = 0.03 \text{ M}$ ,  $m/V = 1.1 \text{ g/L}$ ), and the dotted line (-----,  $I = 0.01 \text{ M}$ ,  $m/V = 1.1 \text{ g/L}$ ) are calculated with Clayeq1. The fitting parameters are the same as in Fig. 3. The inset shows the same data on a different scale.  $R_d^{\text{Ni}} = (\text{moles of Ni adsorbed/mass of dry clay})/(\text{moles of Ni in solution})$ .

tude of these two factors. At high absolute surface charge densities (and potentials), when the net effect of the negative permanent charge inside the clay is relatively unimportant, the effect of decreasing ionic strength is to increase the absolute value of the surface potential, as in the Gouy–Chapman model (see Fig. 6). At high absolute surface charge density, the increase in  $\psi_o$  associated with decreasing  $I$  is in fact about the same in the clay and the Gouy–Chapman models. At small positive potentials, however, decreasing the ionic strength results in a decrease in the surface potential of the clay because the decrease in potential inside the clay (which becomes more negative) is dominant over the decreased shielding in solution.

### Ni and Zn Isotherms

Ni and Zn isotherms were measured by Baeyens and Bradbury (17) at different pH's (see Figs. 7 and 8). No isotherms were obtained for Mn. As expected, for a given concentration in the dissolved phase, the concentration of adsorbed metal increases as the pH increases. The Zn and Ni isotherms show the same features, although data at low concentrations of adsorbed Zn are not available. Ni isotherms show two linear regions, where the slope of the  $\log(\text{Ni}_{\text{ads}})$  vs  $\log(\text{Ni}_d)$  curve is close to 1. If  $\text{Ni}_{\text{ads}} < 2.10^{-3} \text{ mol/Kg}$ , the strong sites are

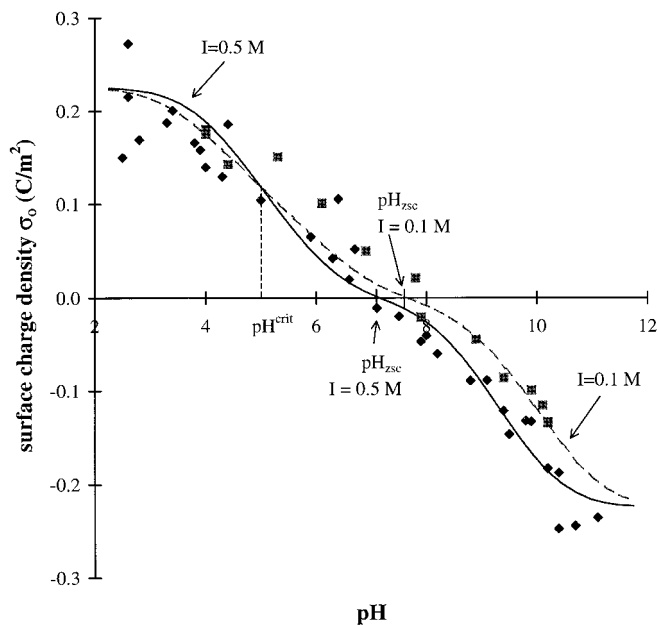


**FIG. 5.** Surface charge density versus pH curves, referred to as titration or potentiometric curves in the text. The squares ( $I = 0.1 M$ ) and the diamonds ( $I = 0.5 M$ ) are data points determined by Baeyens and Bradbury (17). The dotted line ( $I = 0.1 M$ ) and the full line ( $I = 0.5 M$ ) are calculated by Clayeq1 with  $m/V = 6.12$  g/L. The fitting parameters are the same as in Fig. 3.

undersaturated and control the adsorption of Ni. When  $Ni_{ads} > 2 \cdot 10^{-3}$  mol/Kg, the strong sites are saturated and the adsorption is controlled by the weak sites.

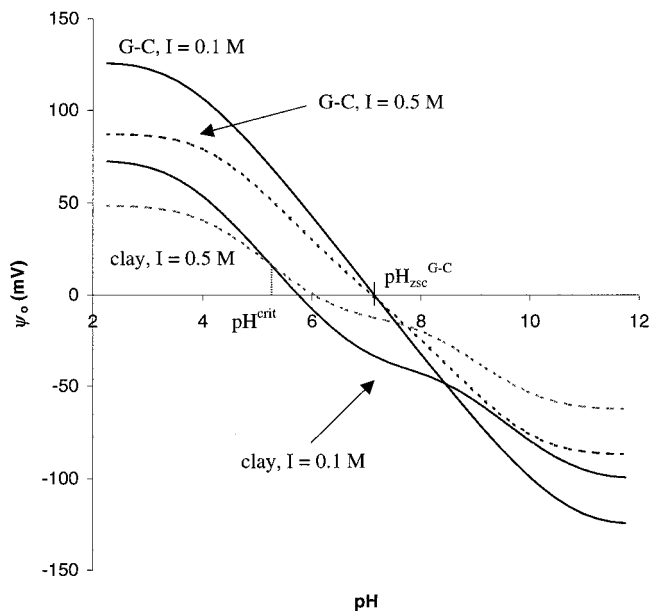


**FIG. 6.** Potential as function of pH at  $I = 0.1 M$  and  $I = 0.5 M$  as calculated by the clay model and the Gouy–Chapman models ( $m/V = 6.12$  g/L). The fitting parameters are the same as in Fig. 3.

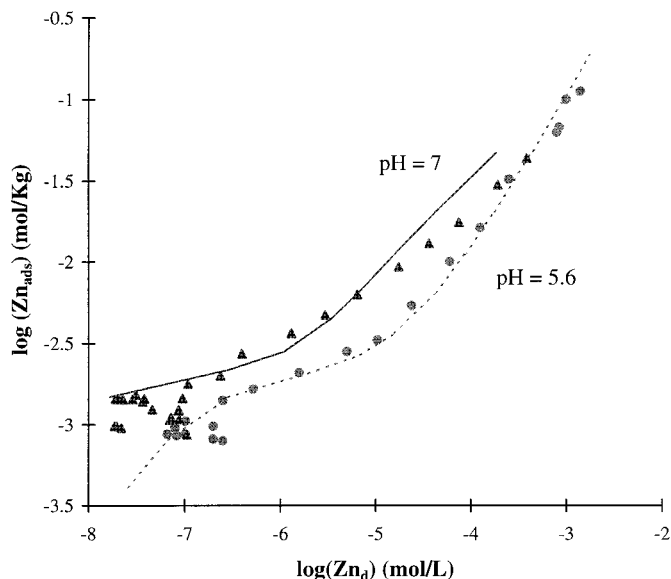


**FIG. 7.** Zn isotherms at two different pHs and  $I = 0.1 M$ . The triangles (pH 7) and the circles (pH 5.6) are from Baeyens and Bradbury (17). The full line (pH 7,  $m/V = 0.325$  g/L) and the dotted line (pH 5.6,  $m/V = 1.16$  g/L) are calculated with Clayeq1. The fitting parameters are the same as in Fig. 3.

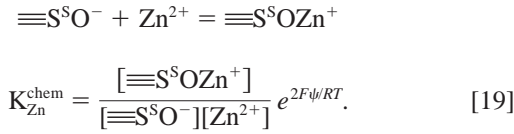
#### Sorption Edges of Zinc, Nickel, and Manganese

The sorption edges of Zn and Ni at  $I = 0.1 M$  show three main regions (see Figs. 3 and 4). The sorption is constant at low pH; it increases at intermediate pH until it reaches a maximum; it then decreases, presumably due to the formation of soluble hydrolysis complexes of Zn and Ni. For Ni, sorption edges were also measured at  $I = 0.03 M$  and  $I = 0.01 M$ . As the ionic strength decreases, the pH-independent component of adsorption becomes increasingly important, until at  $I = 0.01 M$ , the pH-dependent region of the sorption edge has almost disappeared (see Fig. 4). At the total metal concentrations used in the sorption edge experiments, the adsorption is dominated by the strong surface sites, except at high pH where the strong sites begin to be saturated and adsorption on the weak sites comes into play.

Unlike those of Zn and Ni, the sorption of Mn was not studied by Baeyens and Bradbury in a separate set of experiments and there are relatively few data for Mn. The general features of these data (not shown) are, however, similar to the Zn and Ni sorption edges and can be fitted with reasonable model parameters (see Tables 1 and 2).

In the region where adsorption increases with pH, the slope of  $\log(R_d)$  vs pH is lower than 1, which is both unusual and difficult to describe (see insets to Figs. 3 and 4;  $R_d = (\text{moles of metal adsorbed/mass of dry clay})/(\text{moles of metal in solution})$ ). To fit the data, we thus choose to uncouple the acid-base constants of the weak and strong sites. (It should be kept in mind that acid-base constants for the strong sites cannot be

determined experimentally and are thus largely fitting parameters.) If the strong sites are very acidic,  $\equiv\text{S}^{\text{S}}\text{O}^-$  is the major surface species in most of the pH range of interest and the dominant surface complexation reaction (for example with  $\text{Zn}^{2+}$ ) becomes



Differentiation of the mass law [19] with respect to pH results in

$$\frac{d(\log R_d^{\text{Zn}})}{d(\text{pH})} = -\frac{2}{2.3} \frac{F}{RT} \frac{d\psi_0}{d(\text{pH})} = -2\delta. \quad [20]$$

As seen in Fig. 6,  $\psi_0$  decreases as the pH increases and  $\delta$ , the second term of Eq. [20], is negative. In the Gouy–Chapman model, the absolute value of  $\delta$  varies from near unity at low ionic strengths and pHs near the  $\text{pH}_{\text{zsc}}$  to low values at high ionic strengths and pHs far from the  $\text{pH}_{\text{zsc}}$  (25). In the clay

model, because of the influence of the internal potential, the surface potential is less sensitive to the surface charge and  $\delta$  (which is directly proportional to the slope on Fig. 6) is near  $-\frac{1}{2}$ . The clay model thus helps to account for the relatively weak increase in metal adsorption with pH.

The fitting of Ni sorption edges at low ionic strength ( $I = 0.03 \text{ M}$  and  $I = 0.01 \text{ M}$ ) is completely constrained for all parameters and constants have been determined from the other sorption data and are now fixed. As seen in Fig. 4, the model fits the data satisfactorily on the usual % adsorbed vs pH graph, although, as discussed below, there are significant discrepancies on a  $\log(R_d)$  vs pH graph (see inset).

### DISCUSSION

The model for the adsorption of trace cations on clays we have presented is a logical extension of the usual surface complexation model. In this sense, it is certainly parsimonious; if we consider  $\epsilon_c$  and  $V_L/V_P$  as given, only one parameter, the permanent charge per water volume in the clay particle, has been added to the parameters generally used in the surface complexation model as applied to oxides.

Also, while the representation of the clay particle as a homogeneous porous solid is clearly an approximation, the clay model is reasonable, both in its physical and chemical description of the clay and in the values of the parameters that fit the data. In particular, the variations in the surface potential with ionic strength ( $I = 10^{-1} \text{ M}$  to  $I = 10^{-4} \text{ M}$ ) obtained from the clay model and from the more elaborate electrostatic model presented by Secor and Radke (14) are similar. For example, for a montmorillonite with a cation exchange capacity of 0.8 eq/Kg and a surface (edge) charge density of 0.1 C/m<sup>2</sup>, the clay model predicts that the surface potential should decrease by 60 mV when  $I$  decreases from 0.01 to 0.001 M; for the same system, the model of Secor and Radke predicts a decrease in the surface potential of 52 mV. Clearly, the clay model has the advantage of mathematical simplicity as it yields a closed form solution for the surface charge–surface potential relation which can be easily incorporated into a surface complexation model and used to model a wide variety of adsorption data on clays. Whether one model or the other is more appropriate depends on whether the lamellae are best considered in isolation (the interlayers are wider than the double-layer thickness) or as an ensemble constituting a particle. The chemical parameters obtained from fitting the experimental data with the clay model are also consistent with our knowledge of the system. The  $\text{pK}_a$ 's obtained for the acid-base groups at the surface (5.6 and 8.7) are well within the range of typical values for the intrinsic acidity constants of  $\equiv\text{AlOH}$  groups of aluminum oxides (5.2–7.9 and 8.1–10; 29). This might be an indication that only the  $\equiv\text{AlOH}$  groups at the edges of the montmorillonite are reactive; the same conclusion was reached by Wieland and Stumm in their work on kaolinite (30). Also the

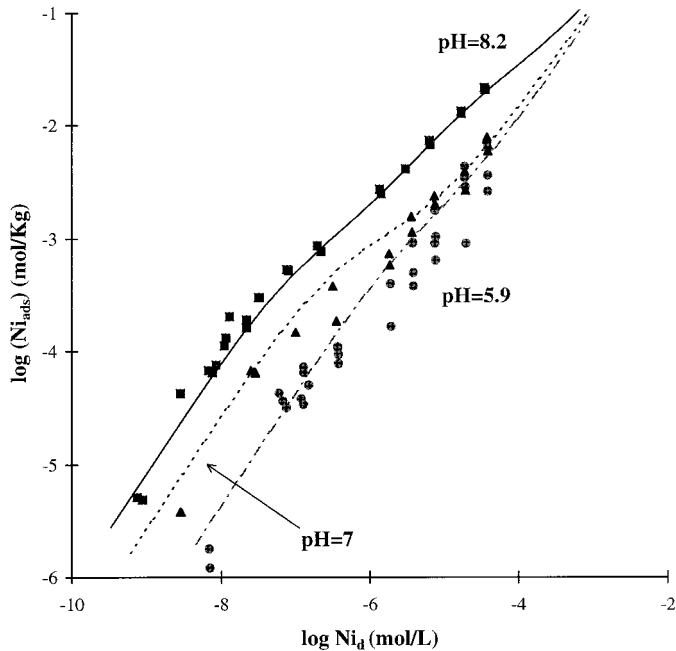


**FIG. 8.** Ni isotherms at three different pHs and  $I = 0.1 \text{ M}$ . The circles (pH 5.9), the triangles (pH 7) and the squares (pH 8.2) are from Baeyens and Bradbury (17). The semi-dotted line (---, pH 5.9,  $\text{m/V} = 0.24 \text{ g/L}$ ), the dotted line (-----, pH 7,  $\text{m/V} = 0.24 \text{ g/L}$ ), and the full line (—, pH 8.2,  $\text{m/V} = 0.24 \text{ g/L}$ ) are calculated with Clayeq. The fitting parameters are the same as in Fig. 3.

relative values of the intrinsic complexation constants  $K^{\text{chem}}$  obtained for Zn, Mn, and Ni are consistent with the order of the first hydrolysis constants:  $K_{\text{ZnOH}} > K_{\text{NiOH}} > K_{\text{MnOH}}$  (31). The model yields to  $K_{\text{Zn}}^{\text{chem}} > K_{\text{Ni}}^{\text{chem}} \sim K_{\text{Mn}}^{\text{chem}}$  (see Table 1). The binding constants for Ni and Mn obtained by the model are similar, but the Mn constant is poorly constrained by the available sorption edge data.

To fully account for the relatively weak dependence of metal adsorption on pH, we uncoupled the acid-base constants of the weak and strong sites and imposed highly acidic strong sites; this is hardly consistent with the rules of coordination chemistry. Another option yielding a good fit of the metal sorption edges is to include in the model an unusual surface species such as  $\equiv\text{SOHZn}^{2+}$ . (Indeed,  $\equiv\text{SOHMe}^{2+}$  surface species have been used before to model metal sorption on hydrous ferric oxide and clays; 12, 25). It allows the model to fit the data with fewer parameters, because the acid-base constants are kept the same for the weak and strong sites. Experimental evidence for the existence of surface complexes such as  $\equiv\text{SOHZn}^{2+}$  is lacking, however. The answer to this puzzle may lie in the two distinct types of surface sites,  $\equiv\text{SiOH}$  and  $\equiv\text{AlOH}$ , that coexist on the clay edge; both would have to be taken into account in a chemically realistic model. We made some computer simulations with a model such that  $\equiv\text{SiOH}$  groups deprotonate to give  $\equiv\text{SiO}^-$  at pHs below those where  $\equiv\text{AlOH}_2^+$  sites lose their protons to yield  $\equiv\text{AlOH}$  (32), neither  $\equiv\text{SiOH}_2^+$  nor  $\equiv\text{AlO}^-$  being ever significant. We found that this model, using reasonable constants for  $\equiv\text{SiOH}$  and  $\equiv\text{AlOH}$  surface groups (29), could provide an acceptable fit of both the titration and sorption edge data. This model is mathematically very similar to the one we have presented here, in which we chose instead, in keeping with the tradition of surface complexation models, the formalism of only one diprotic surface group.

To decide whether our clay model provides a truly appropriate description of adsorption on clays, it is not sufficient that it be parsimonious and reasonable, however; it must also allow us to model features of the experimental data that are specific to clays and be difficult or impossible to model otherwise. There are three such features: the adsorption of cations at low pHs, the low slope of  $\log(R_d)$  vs pH graph, and the variations in  $\text{pH}_{\text{zsc}}$  with  $I$ .

First, a characteristic of clays is the sizable adsorption of trace cations at low pHs and its variations with ionic strength. Previously, cation exchange reactions were accounted for in surface complexation models by assuming the formation of highly stable complexes between the permanently charged surface groups and the cations. Clearly, the formation of such stable complexes is an ad-hoc assumption which lacks chemical or structural justification. Further, as pointed out before, it is problematic to describe cation exchange, which results from the electrostatic attraction of the cations by the permanent

charge of the clay, by way of a specific chemical reaction. In contrast, the clay model is able to describe cation exchange as a purely electrostatic process as the cations are attracted by the negative potential inside the clay particle.

Second, the clay model correctly predicts the weaker (compared to oxides) pH dependence of metal adsorption on clays (i.e., the low slopes of the  $\log(R_d)$  vs pH graphs). These low slopes may be reproduced by ad-hoc means such as setting the coulombic term to zero (10). As discussed earlier, the success of the clay model in describing the appropriate dependency of  $R_d$  on pH reflects the lesser dependency of  $\psi_o$  on pH that results from the built-in charge-potential relation (Eqs. [9]–[11]), compared to what is predicted by the Gouy–Chapman model. The internal negative charge results in a decreased sensitivity of the surface potential to the variations in the surface charge density.

Finally, and probably most important, is the ability of the clay model to reproduce the variations in  $\text{pH}_{\text{zsc}}$  with ionic strength and the increase in  $\text{H}^+$  adsorption with decreasing ionic strength that are seen in the potentiometric data (33). The Gouy–Chapman model (or its variations) always predicts that all the acid-base titration curves should intercept at a fixed  $\text{pH}_{\text{zsc}}$ , independent of  $I$  and that, at a given pH, the absolute value of the surface charge should always decrease with decreasing  $I$ . In surface complexation models applied to clays, the increase in the  $\text{pH}_{\text{zsc}}$  is usually accounted for by introducing a competition between the electrolyte cation (e.g.,  $\text{Na}^+$ ) and  $\text{H}^+$  for the permanently charged groups (34–36). To fit the data, however, the constant for the reaction is fixed at values that vary widely depending on the study and are markedly different from 1—which is in direct contradiction with independent measurements of ion exchange on montmorillonite (6, 37). The clay model, in contrast, predicts that the change in the internal potential of the clay particle due to variations in  $I$  should be reflected in variations in the  $\text{pH}_{\text{zsc}}$ . More precisely, the increase in (negative) internal potential resulting from a decrease in the ionic strength is predicted to sometimes dominate over other electrostatic effects and to result in an increased positive surface charge.

There is one feature of the Baeyens and Bradbury's data that is not well reproduced by the model: the constant maximum Ni adsorption (ca. pH 9–10) with decreasing ionic strength from 0.1 to 0.01 M. Although on a % Ni adsorbed vs pH graph the fits look satisfactory, a  $\log(R_d^{\text{Ni}})$  vs pH graph clarifies the discrepancy between the data and the model at high pH (see inset to Fig. 4). The data show a constant adsorption at high pH when  $I$  decreases, while the model predicts an increase in the adsorption at high pH, mainly due to the decreased shielding of the negative surface charge when  $I$  decreases. For the same reasons, a classic Gouy–Chapman model would likewise fail to reproduce the data.

It may be that this discrepancy is due to the swelling of

montmorillonite with decreasing ionic strength, which is well documented (38–40) but is not taken into account in the model. It is likely that the clay has undergone at least some osmotic (“extensive”) swelling between  $I = 0.1 M$  and  $I = 0.01 M$ . Such swelling should have two effects: (1) experimentally it would make the separation of the clay from the solution by centrifugation increasingly difficult; and (2) it would decrease the internal charge density and increase the surface area of the edges (both effects tending to balance out the increased attraction of the metal by the surface due to decreased shielding). It should be kept in mind that at high pHs, where the discrepancy between model and data is observed, more than 95% of the metal is adsorbed on the clay particles. At this stage, any contamination of the solution phase (where the metal concentration is measured) with the particulate phase is critical. In a few model simulations we took swelling into account by decreasing the internal charge density,  $\rho_{\text{clay}}$ , by a factor of three and increasing the specific surface area by the same factor when decreasing the ionic strength from  $I = 0.1 M$  to  $I = 0.01 M$ . The discrepancy between model and data was reduced significantly, but the model still predicted an increase in  $\log(R_d)$  when  $I$  decreases at high pH.

## CONCLUSION

Overall, the clay model provides a reasonable and parsimonious description of the acid-base and cation sorption properties of Na-montmorillonite. Moreover, the differences in the surface charge-surface potential relation of the clay model compared to the Gouy–Chapman model appear important in modeling some specific aspects of experimental adsorption data on clays. Besides data fitting, the clay model is useful in providing an insight into the effects of the permanent charge on the reactivity of surface sites as a function of ionic strength. Clearly, the simple clay adsorption model we have presented may need to be modified to account for the particularities of various smectites. For example, reactive sites in the interlayers may undergo proton exchange reactions or exhibit specific chemical affinity for some sorbates. Or swelling may indeed have to be described quantitatively. Nonetheless we hope that the general model we have presented will provide a template, a “metamodel,” from which other models of sorption on montmorillonite may be patterned. Besides its apparent applicability to at least one particular data set, the strength of this general model rests with its self-consistency. Since ion exchange in the clay is primarily a coulombic process, it is satisfying that its quantitative description be made consistent and interdependent with the coulombic effects on the edge surfaces. In a most general way, what the clay model does is simply to extend the Gouy–Chapman model on the other side of the interface, into the interior of the hydrated clay particle, by solving the Pois-

son–Boltzmann equation in the whole instead of half of space. This would seem a useful approach to describe the interactions of solutes with any penetrable solid.

## ACKNOWLEDGMENTS

The authors thank Janet G. Hering, Bettina M. Voelker, and James J. Morgan for their helpful comments, as well as William Schecher for his assistance with Mineql +3.0. Financial supports from E.P.A., N.S.F., O.N.R., and I.F.R.E.M.E.R. are gratefully acknowledged.

## REFERENCES

1. Dzombak, D. A., and Hudson, R. J. M., in “Aquatic Chemistry: Interfacial and Interspecies Processes” (C. P. Huang, C. R. O’Melia, and J. J. Morgan, Eds.), p. 59. American Chemical Society, Washington DC, 1995.
2. Zachara, J. M., and McKinley, J. P., *Aquat. Sci.* **55**, 250 (1993).
3. McKinley, J. P., Zachara, J. M., Smith, S. C., and Turner, G. D., *Clays and Clay Minerals* **43**, 586 (1995).
4. Morris, D. E., Chisholm-Brause, C. J., Barr, M. E., Conradson, S. D., and Eller, P. G., *Geochim. Cosmochim. Acta* **58**, 3613 (1994).
5. Bolt, G. H., in “Soil Chemistry. B. Physico-Chemical Models” (G. H. Bolt, Ed.) Elsevier, Amsterdam, 1979.
6. Fletcher, P., and Sposito, G., *Clay Miner.* **24**, 375 (1989).
7. Schindler, P. W., Furst, B., Dick, R., and Wolf, P. U., *J. Colloid Interface Sci.* **55**, 469 (1976).
8. Davis, J. A., James, R. O., and Leckie, J. O., *J. Colloid Interface Sci.* **63**, 480 (1977).
9. Hayes, K. F., and Leckie, J. O., *J. Colloid Interface Sci.* **115**, 564 (1987).
10. Bradbury, M. H., and Baeyens, B., *J. Cont. Hydro.* **27**, 223 (1997).
11. Charlet, L., Schindler, P. W., Spadini, L., Furrer, G., and Zysset, M., *Aquat. Sci.* **55**, 291 (1993).
12. Stadler, M., and Schindler, P. W., *Clays and Clay Minerals* **41**, 288 (1993).
13. Zachara, J. M., Smith, S. C., McKinley, J. P., and Resch, C. T., *Soil Sci. Soc. Am.* **57**, 1491 (1993).
14. Secor, R. B., and Radke, C. J., *J. Colloid Interface Sci.* **103**, 237 (1985).
15. Chang, F.-R. C., and Sposito, G., *J. Colloid Interface Sci.* **178**, 555 (1996).
16. Chang, F.-R. C., and Sposito, G., *J. Colloid Interface Sci.* **163**, 19 (1994).
17. Baeyens, B., and Bradbury, M. H., *J. Cont. Hydro.* **27**, 199 (1997).
18. Lyklema, J., *J. Electroanal. Chem.* **18**, 341 (1968).
19. Perram, J. W., Hunter, R. J., and Wright, H. J. L., *Chem. Phys. Lett.* **23**, 265 (1973).
20. Perram, J. W., Hunter, R. J., and Wright, H. J. L., *Aust. J. Chem.* **27**, 461 (1974).
21. Verwey, E. J. W., and Niessen, K. F., *Phil. Mag. (7)* **28**, 435 (1939).
22. Grimley, T. B., and Mott, N. F., *Discussions Faraday Soc.* **1**, 3 (1947).
23. Grimley, T. B., *Proc. Roy. Soc. London A* **201**, 40 (1950).
24. Bartschat, B., Cabaniss, S. E., and Morel, F. M. M., *Environ. Sci. Technol.* **26**, 284 (1992).
25. Dzombak, D. A., and Morel, F. M. M., “Surface Complexation Modeling,” Wiley-Interscience, New York, 1990.
26. McBride, M. B., “Environment Chemistry of Soils,” Oxford University Press, Oxford, 1994.
27. Sposito, G., “The Surface Chemistry of Soils,” Oxford University Press, New York, 1984.
28. Rutherford, D. W., Chiou, C. T., and Eberl, D. D., *Clays and Clay Minerals* **45**, 534 (1997).
29. Schindler, P. W., and Stumm, W., in “Aquatic Surface Chemistry” (W. Stumm, Ed.), p. 83. Wiley-Interscience, New York, 1987.

30. Wieland, E., and Stumm, W., *Geochim. Cosmochim. Acta* **56**, 3339 (1992).
31. Baes, C. F., and Mesmer, R. E., "The Hydrolysis of Cations," Wiley, New York, 1976.
32. Lyklema, J., "Fundamentals of Interface and Colloid Science. Vol. II: Solid-Liquid Interfaces," Academic Press, London, 1993.
33. Kraepiel, A. M. L., Keller, K., and Morel, F. M. M., *Environ. Sci. Technol.* **32**, 2829 (1998).
34. Avena, M. J., and De Pauli, C. P., *J. Colloid Interface Sci.* **202**, 195 (1998).
35. Schindler, P. W., Liechti, P., and Westall, J. C., *Neth. J. Agr. Sci.* **35**, 219 (1987).
36. Wanner, H., Albinsson, Y., Karnland, O., Wieland, E., Wersin, P., and Charlet, L., *Radiochim. Acta* **66/67**, 157 (1994).
37. James, R. O., and Parks, G. A., *Surf. Colloids Sci.* **12**, 119 (1982).
38. Norrish, K., *Discussions Faraday Soc.* **18**, 120 (1954).
39. Quirk, J. P., and Marcelja, S., *Langmuir* **13**, 6241 (1997).
40. Zhang, F., Low, P. F., and Roth, C. B., *J. Colloid Interface Sci.* **173**, 34 (1995).